

# Self-consistent simulation of local potential in external-gate biased graphene nanoribbons

*Davide Mencarelli<sup>1</sup>, Tullio Rozzi<sup>1</sup>, Luca Pierantoni<sup>1</sup>, Fabio Coccetti<sup>2</sup>*

<sup>1</sup>Dipartimento di Ingegneria Biomedica, Elettronica e Telecomunicazioni,  
Università Politecnica delle Marche Ancona, Via Brecce Bianche 12, 60131, Italy, [l.pierantoni@univpm.it](mailto:l.pierantoni@univpm.it)

<sup>2</sup>Laboratoire d'Analyse et d'Architecture des Systèmes-Centre National de la Recherche Scientifique (LAAS-CNRS),  
Micro and Nanosystems for Wireless Communications, Avenue du Colonel Roche 7, Toulouse, 31077 France,  
[coccetti@laas.fr](mailto:coccetti@laas.fr)

## Abstract

We report on the self-consistent analysis of armchair graphene nanoribbon (GNR) field-effect transistors (FET), in the case of multi-band coherent carrier transport. In principle, the same approach can be extended to include the contribution to charge transport due to different layers of a few-layer GNR-FET. To the aim of demonstrating the versatility of our simulation tool, we provide interesting examples about the dependence of charge and self-consistent potential on the gate voltage, for small drain voltages: these include details of numerical convergence of the iterative system of Poisson and Schrödinger equations.

## 1. Introduction

In recent years, the technological relevance of graphene, made of carbon atoms packed in a 2D-honeycomb lattice, has been highlighted in the literature: graphene is likely to become competitive and compatible with the established silicon technology for applications to electronics.

Our analysis is focused on graphene nanoribbons (GNR), that is, narrow strips of graphene. The importance of this issue is reflected by a variety of works, both experimental [1-4] and theoretical [5-7]. The analysis of GNR can be carried out by a variety of models, [8-11], able to solve, in principle, even complicated problems such as, for example, the effects on charge transport of applied external electric and magnetic fields [12], bending [13], lattice defects, discontinuities, and edge terminations [14], and so on. The reasons for the success of these models reside in that they make use of quite good and well verified assumptions, two in particular: - transport is ballistic due to low-dimensionality and high purity of carbon lattice, - electron interaction is weak owing to the relatively long distances involved in charge displacement. In fact, we are not dealing with molecular devices, where the above assumptions may not hold and a Fock-space picture of quantum channels may be needed. Using *ab initio* density functional theories, where the bands are filled self consistently, may be necessary when fine effects are to be highlighted, such as, for example, a detailed description of electronic dispersion of GNR around the Fermi level. However the latter methods requires high computational resources, and can hardly include external electric fields.

We make use of a multimode approach to quantum transport, allowing easy simulation of very large structures, despite the possibly high number of electronic channels involved. The linear charge and the current are computed by solving separately the Schrödinger equation for any sub-band, each one with its respective effective masses. However, even though the wavefunctions of different channels are not spatially coupled, they are coupled through the Poisson equation, since they all contribute to the source charge for the self consistent potential.

At the chosen low energies, the contribution of the sub-bands is very small but this does not lower the generality of the approach.

## 2. GNR-FET modelling

We start by recalling the basic points of the approach widely used, in the literature, in analysing the behaviour of a single-wall CNT surrounded by a cylindrical gate electrode and with left/right terminations contacted by source/drain. A self consistent solution of the system of Poisson and Schrödinger equations directly provides both the linear charge along the GNR, which is considered as wire of negligible thickness, and the electrostatic potential along the GNR:

$$\left\{ \begin{array}{l} \frac{d^2V}{d\rho^2} + \frac{1}{\rho} \frac{dV}{d\rho} + \frac{dV}{dz^2} = -\frac{Q}{\epsilon} \end{array} \right. \quad (1)$$

$$\left\{ \begin{array}{l} \frac{d^2\Psi_{h,e}}{dz^2} = -\frac{2m}{\hbar^2} (E - U_{h,e}) \Psi_{h,e} \end{array} \right. \quad (2)$$

where  $V$  is the electrostatic potential,  $\psi$  is the z-dependent wave-function of a hole (electron) of energy  $E$ , travelling under the effect of a local potential energy  $U_h$  ( $U_e$ ),  $Q$  is the nanotube linear charge density, which is given by the difference between electron and hole charges, diffused from drain and source,  $m$  is the appropriate effective mass of the considered band. We refer to the gate-source and drain-source voltages as  $V_{gs}$  and  $V_{ds}$  respectively. A self-consistent solution of the equations (1) and (2) is achieved when

$$V(Q) = V, \quad Q(V) = Q \quad (3)$$

Here the symbol “=” indicates the convergence of an iterative scheme, that is reached when charge and potential differ from their values calculated at the previous step by less than a very small percentage. The Landauer-Büttiker formula is used to calculate the total current flowing through the GNR:

$$I_{h,e} = -\frac{4e}{h} \int (f_{h,e}^s - f_{h,e}^d) T_{h,e} dE \quad (4)$$

In (4),  $e$  is the electron (hole) unit charge for  $I_e$  ( $I_h$ ),  $h$  is the Plank's constant,  $T_e$  ( $T_h$ ) is the transmission probability through the channel for the electrons (holes) and  $f_{h,e}^{s,d}$  is the Fermi function at the source and drain.

As already mentioned, the above model is extended here to include the contribution of any sub band. Only electron transport is considered here: the device under test is not of the schottky type as, in fact, the metal contact is assumed to slightly change the Fermi level of the GNR, and the electron affinity is the same everywhere.

In the present work we report the example of a two-port GNR of  $12 \times 208$  atoms in a FET configuration. The latter is shown in Fig. 1, together with its dispersion curves. Note that the GNR is semiconducting with band gap of about 0.6 eV. The dispersion curves have been plotted only for positive energies since the negative ones show a symmetric dependence. The same holds for  $ka$ , that ranges only from 0 to 180 degrees because the negative angles shows a symmetric behavior.

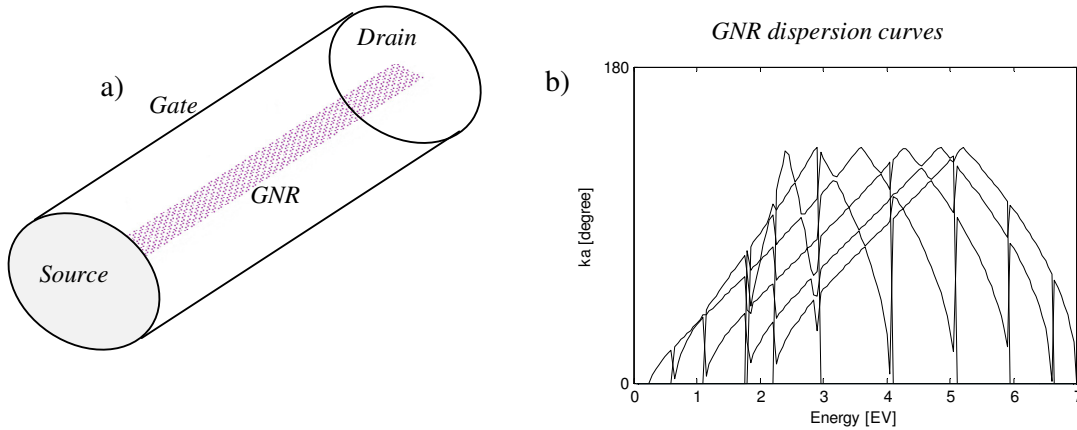


Fig. 1. a) GNR channel; b) dispersion curves of the simulated GNR channel, the jumps to zero are just numerical jumps from one curve to one other.

In the present example, the Fermi level in the contacted GNR is assumed to be 360 meV. In Fig 1a we report the iterative convergence of the potential curve for a fixed  $V_{gs}=0.02V$  and  $V_{ds}=0$ . The dependence of the potential curves on  $V_{gs}$  (and  $V_{ds}=0$ ) is shown in Fig .2b and refer to the last iterative step, when numerical convergence is obtained.

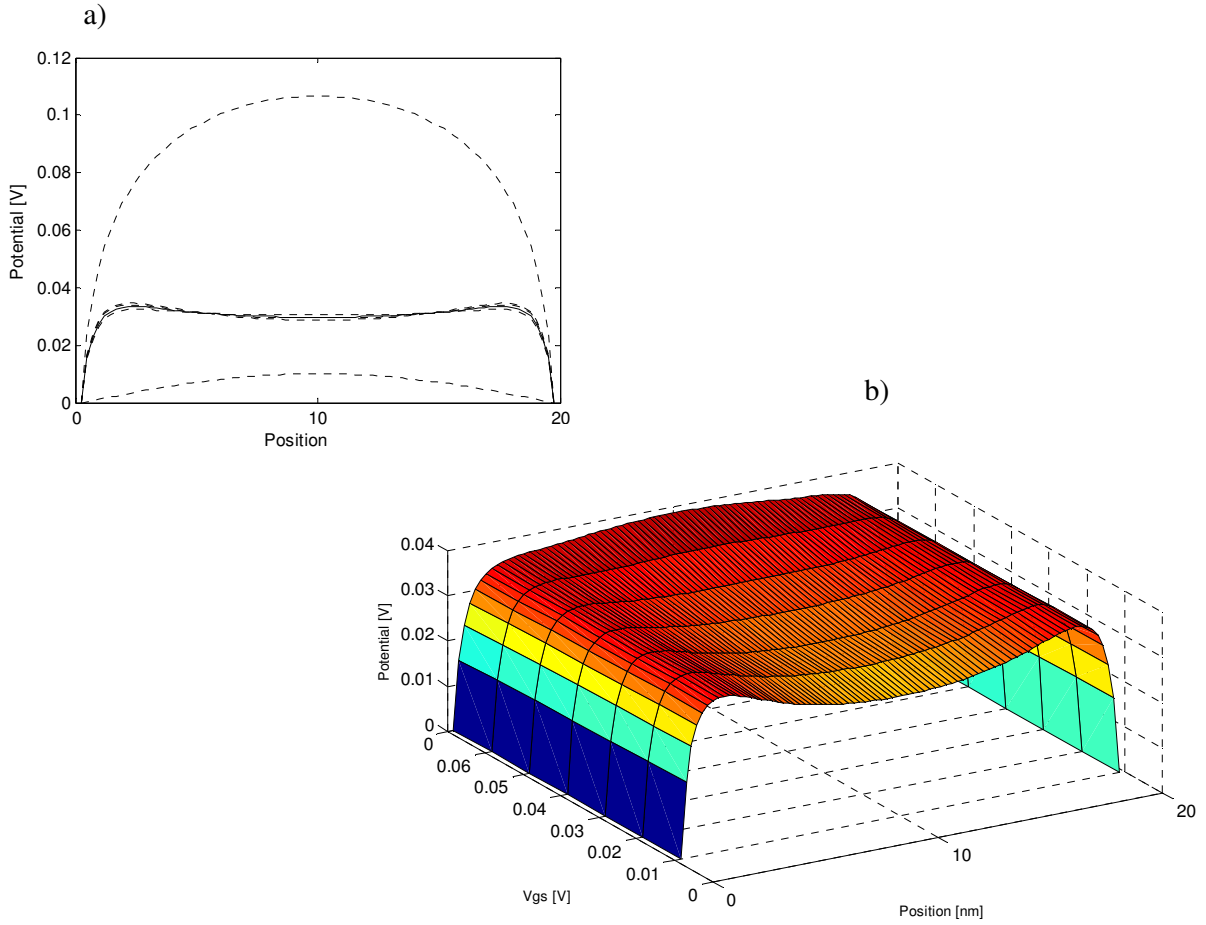


Fig. 2 a) Numerical convergence of the electrostatic potential along the GNR,  $V_{gs}=0.02$  V,  $V_{ds}=0$ ; the dot lines represent intermediate steps of the iterative calculation, whereas the solid line is the final converging curve; b) dependence of the self-consistent local potential on the gate voltage  $V_{gs}$ .

The applied iterative scheme requires a starting function for the potential, or for the charge, as close as possible to the final solution, in order to avoid numerical divergence. In fact, the main issue in simulating complex devices is given by the handling of the non-linear Poisson-Schrödinger system. There is never any “a priori” guarantee that the iterative approach will actually converge to a stable solution: this is a rather common and well known limit cycle problem, occurring when a particular charge density ( $Q_a$ ) gives rise to a certain potential ( $V_a$ ) and, in the next numerical cycle, a different pair ( $Q_b$ ) and ( $V_b$ ) is produced, so that charge and potential simply bounce back and forth from state (a) to state (b) states, never converging. Thus, a particular care is required when handling equations (1) and (2); in the above figure we have shown some successful simulation examples.

### 3. Conclusion

In this contribution we report on numerical simulation of graphene-nanoribbon based transistors. In particular we characterize the use of a single layer GNR as channels for charge transport and evaluate, in a self-consistent charge-potential framework, the dependence of local potential on an external applied voltage, with emphasis to the numerical features of the implemented iterative algorithm.

## 4. References

1. Z. Chen, Y.-M. Lin, M. J. Rooks and P. Avouris, "Low-dimensional Systems and Nanostructures" *Physica E* Volume 40, Issue 2, pages 228-232, Dec. 2007.
2. M. Y. Han, B. Özyilmaz, Y. Zhang, and P. Kim, "Energy Band-Gap Engineering of Graphene Nanoribbons" *Phys. Rev. Lett.* 98, 206805, 2007.
3. X. Li, et al., "Chemically Derived, Ultrasmooth Graphene Nanoribbon Semiconductors" *Science* 319, 1229, 2008.
4. C. Stampfer, J. Güttinger, S. Hellmüller, F. Molitor, K. Ensslin, and T. Ihn, "Energy Gaps in Etched Graphene Nanoribbons", *Phys. Rev. Lett.* 102, 056403, 2009.
5. X. Liu, J. B. Oostinga, A. F. Morpurgo, and L. M. K. Vandersypen, "Electrostatic confinement of electrons in graphene nanoribbons", *Phys. Rev. B* 80, 121407(R), 2009.
6. K. Wakabayashi and M. Sigrist, "Zero-Conductance Resonances due to Flux States in Nanographite Ribbon Junctions", *Phys. Rev. Lett.* 84, 3390–3393, 2000.
7. S. Souma, M. Ogawa, T. Yamamoto and K. Watanabe, "Numerical Simulation of Electronic Transport in Zigzag-edged Graphene Nano-Ribbon Devices", *J. of Computational Electronics*, vol. 7, n.3, 390-393, 2008.
8. L. Brey and H. A. Fertig, Electronic States of Graphene Nanoribbons, *cond-matt.* 0603107, 5 Mar 2006.
9. Y. Ouyang, Y. Yoon; J. Guo, "Scaling Behaviors of Graphene Nanoribbon FETs: A Three-Dimensional Quantum Simulation Study" *IEEE Transactions on Electron Devices*, 54, Issue 9, 2223 – 2231, 2007
10. Z. F. Wang, R. Xiang, Q. W. Shi, J. Yang, X. Wang, J. G. Hou and J. Chen, "Modeling STM images in graphene using the effective-mass approximation", *Phys. Rev. B* 74, 125417, 2006.
11. T. Ando, "Quantum point contacts in magnetic fields", *Physical Review B* 44, 8017, 1991.
12. E. V. Castro, N. M. R. Peres and J. M. B. Lopes dos Santos, "Gaped graphene bilayer: disorder and magnetic field effects", *Phys. Stat. Sol. (b)* 244, n. 7, 2311–2316, 2007.
13. A. Rycerz, "Nonequilibrium valley polarization in graphene nanoconstrictions", *Phys. stat. sol. (a)* 205, 1281-89 2008.
14. A. R. Akhmerov and C. W. J. Beenakker, "Boundary conditions for Dirac fermions on a terminated honeycomb lattice", *Cond-mat.mes-hall*, 0710.2723v1, 2008.